

1 **Economic Damages of Delayed Climate Action**

2 *By* KENT D. DANIEL, ROBERT B. LITTERMAN, AND GERNOT WAGNER*

3 Draft: December 21, 2025

Delayed climate mitigation imposes substantial economic costs by shifting the burden of adjustment onto future generations. We quantify these welfare losses within a climate-economy model that allows us to calculate the dead-weight loss (DWL) of underpricing carbon pollution. We simulate policy delay by constraining initial mitigation years and comparing resulting welfare outcomes to an unconstrained baseline. We show analytically that delay raises the required expected entry carbon price. Across scenarios, expected
4 *re-entry prices are higher by roughly 0.4-0.9% per additional year of delay. The consumption-equivalent DWL even for short delays of 5 to 15 years ranges from 14-32% of first-period consumption, or roughly \$8-19 trillion (2020 USD) in one-time compensation. DWLs rise steeply but concavely in the length of delay, reflecting catch-up pricing and abatement once the constraint lifts.*

JEL: D62,G12,Q54

Keywords: climate risk, climate policy, cost of carbon

5 Climate economics is, at its core, the economics of delaying optimal choice. Con-
6 sequences of delaying climate mitigation are profound and quantifiable, as every
7 year without meaningful reductions in greenhouse gas emissions increases their
8 concentration and commits the world to higher temperature and greater climate
9 damages. From an economic perspective, these delays are an implicit transfer of

* Daniel: Columbia Business School, New York, NY 10027; Litterman: Kepos Capital, New York, NY 10036; Wagner: Columbia Business School, New York, NY 10027; gwagner@columbia.edu. We thank Theo Moers for excellent research assistance, and participants in the 2025 Dialogues in Complexity Workshop at Princeton University for thoughtful comments.

10 welfare from future generations to the present, an intertemporal reallocation that
11 is driven not by efficiency but political and institutional frictions. Understanding
12 the dynamics of this delay and quantifying the resulting dead-weight loss (DWL)
13 is essential in understanding the true cost of inaction.

14 Most climate-economic integrated assessment models (IAMs) seek to identify
15 the optimal mitigation path that maximizes intertemporal social welfare under
16 a set of assumed parameters. Yet governments rarely, if ever, follow the paths
17 that economists identify as socially optimal. Corporate lobbying (Oreskes and
18 Conway, 2011) and other interest-group politics (Mildenberger, 2020), in part via
19 public opinion (Dechezleprêtre et al., 2025; Mildenberger and Tingley, 2019), in-
20 stitutional constraints (Bertram et al., 2024), behavioral barriers (Wagner and
21 Zeckhauser, 2012), and other political economy considerations (Meckling, Sterner
22 and Wagner, 2017; Meckling, 2025) defer action, even when — or perhaps espe-
23 cially when — the social planner’s problem is well understood.¹

24 The more explicit the attempt at pricing the negative climate externality, the
25 louder are the voices of vested interests lobbying against climate policy. This
26 delay in climate action moves the world further off the efficient frontier, which
27 does not just lead to greater economic damages reflected in higher social cost of
28 carbon (SCC) calculations (Moore et al., 2024), but in measurable DWLs.

29 Here we examine these costs explicitly. Building on a carbon asset pricing
30 framework (Bauer, Proistosescu and Wagner, 2024), which extends the Epstein–Zin
31 recursive preference structure of Daniel, Litterman and Wagner (2019), we quan-
32 tify DWLs of delaying optimal policy by comparing carbon price paths under
33 constrained and unconstrained conditions, analyzing sensitivities of various model
34 parameters, including technological progress and learning. In contrast to Daniel,
35 Litterman and Wagner (2019), we further show that the optimal expected carbon
36 price in a delayed scenario will be higher under standard assumptions than in an

¹It is also what makes *ex-post* analyses of existing policies so fraught (Stechemesser et al., 2024): Policies that get enacted are necessarily limited in scope and strength.

unconstrained scenario.

We present simple heuristics about the high and quickly accumulating costs of delayed climate action, finding DWLs of delay of between 14-32% of first-period consumption, or \$8-19 trillion (2020 USD), even for relatively short delays of between 5 and 15 years. These numbers compare to cost estimates of between \$400 and \$900 per household (Clausing, Knittel and Wolfram, 2025) and are significantly higher than typically calculated, using SCC-based measures. The optimal carbon price in our base case here is roughly \$200, above the median value of around \$185 of Moore et al. (2024)’s “synthetic distribution” yet well below its mean SCC of around \$280. Meanwhile, Bilal and Känzig (2025) calculate an SCC above \$1500 and a welfare cost of (only) around 30%. A key difference to our analysis: we solve for the ‘optimal’ carbon price by considering marginal disutility of damages, instead of calculating the SCC, the discounted value of the stream of expected future damages.

I. Socio-economic modeling choices

To explore how postponing climate policy affects welfare and the socially optimal carbon price path, we endow a representative agent with recursive Epstein-Zin (EZ) preferences and place it within a binomial decision tree where utility is maximized at each step. Such preferences allow us to disentangle risk over time from risk across states of nature. This distinction follows Epstein and Zin (1989, 1991), with a long history in financial economics, and a more recent one in modeling the financial implications of climate risks (Ackerman, Stanton and Bueno, 2013; Traeger, 2014; Lemoine and Traeger, 2014).

The representative agent’s preferences follow the recursive Epstein–Zin specification,

$$(1) \quad U_t = \left((1 - \beta)c_t^\rho + \beta[\mathbb{E}_t(U_{t+1}^\alpha)]^{\rho/\alpha} \right)^{1/\rho},$$

where $\beta := (1 + \delta)^{-1} > 0$ is the one-year discount factor, with $\delta > 0$ denoting the pure rate of time preference; $c_t > 0$ is consumption at time t ; $\rho := 1 - 1/\sigma$, where $\sigma > 0$ is the elasticity of intertemporal substitution (EIS); and $\alpha := 1 - \gamma$, where $\gamma > 0$ is the coefficient of relative risk aversion (RA). The term $\mathbb{E}_t(U_{t+1}^\alpha)$ represents the certainty equivalent of future utility.

When $\alpha = \rho$, that is, when risk aversion and intertemporal substitution coincide, the recursive formulation in Equation (1) collapses to the standard time-additive expected-utility form with constant relative risk aversion.

For the terminal period T , we assume exogenous consumption growth $g > 0$ and define terminal utility as

$$(2) \quad U_T = \left[\frac{1 - \beta}{1 - \beta(1 + g)^\rho} \right]^{1/\rho} c_T.$$

This specification cleanly separates two central preference parameters: σ , which governs willingness to substitute consumption over time, and γ , which governs aversion to risk across uncertain future states.²

II. Optimization

Following Daniel, Litterman and Wagner (2019) and Bauer, Proistosescu and Wagner (2024), we embed the representative agent in a finite-horizon probability landscape. Our model has six decision times T_0, \dots, T_5 (Figure 1). At every node (t, s) of the tree, the agent maximizes EZ utility in (1) and chooses a node-specific mitigation level $m_{t,s} \in [0, \bar{m}]$ with upper mitigation bound \bar{m} , subject to climate dynamics, resource constraints, abatement costs, climate damages, and the technological feasibility of mitigation. Each choice commits the agent to a continuation policy for all downstream nodes in a given branch.

The climate state evolves according to the impulse response function (IRF) of Joos et al. (2013) for atmospheric CO_2 concentration C and the TCRE map-

²See Appendix A.A1 for parameter values used in our main specification.

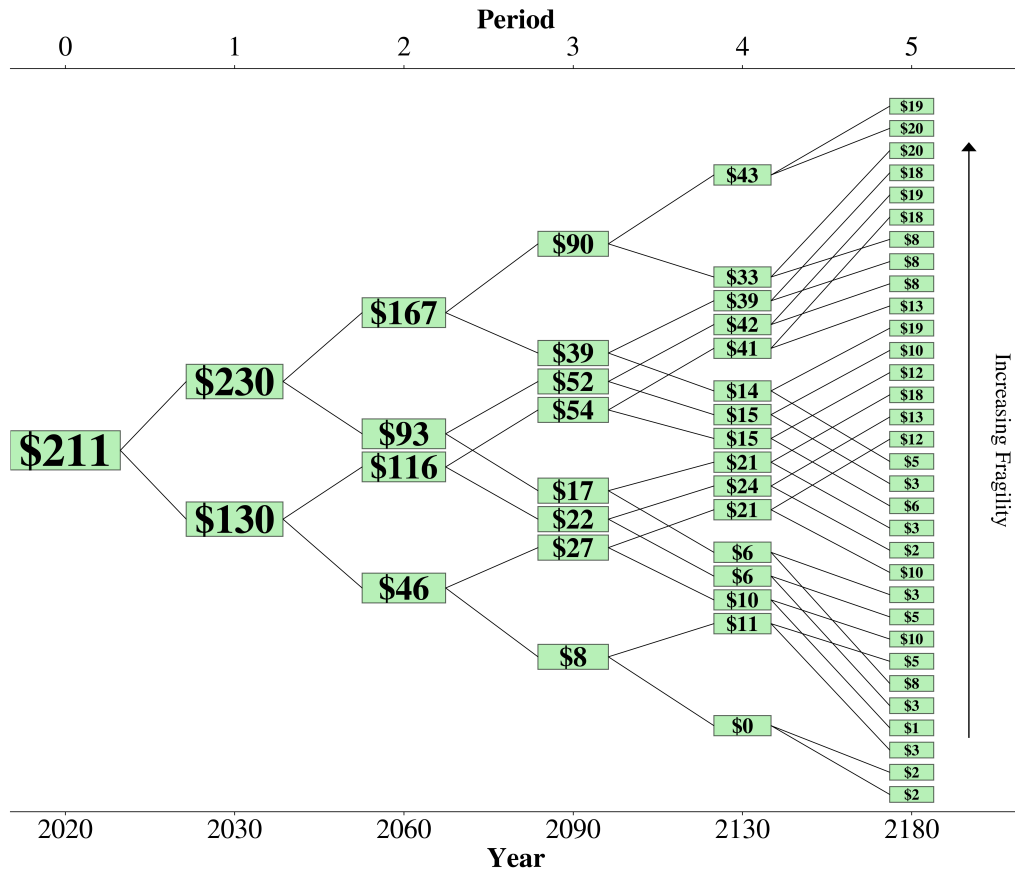


Figure 1. : Optimal price paths (unconstrained baseline)

Note: The binomial non-recombining tree shows the optimal node-level shadow-price trajectory on the stochastic decision tree used in the model. Each node represents a shadow price (in 2020 USD per ton CO₂) at the beginning of the indicated year, conditional on previous realizations of climate and economic uncertainty.

ping from cumulative emissions to the global mean surface *temperature anomaly* θ (in °C above preindustrial), see Eqs. (A2)–(A3) in Appendix A.A1. Our implementation uses a carbon cycle model with persistent parameters from Joos et al. (2013) and uncertain effective TCRE $\lambda_{\text{eff}} \sim \mathcal{N}(0.52, 0.21^2)$. For analytical results we employ a stylized finite-dimensional representation that preserves the key monotonicity properties.

Define at node (t, s) the marginal willingness to pay $\Phi_{t,s}(\theta_{t,s})$ to avoid one additional ton of CO₂ emitted in $[T_t, T_{t+1})$. Mitigation has node-specific marginal cost $\kappa'_{t,s}(m_{t,s}, L_{t,s}) = \partial \kappa_{t,s}(m_{t,s}, L_{t,s}) / \partial m_{t,s}$.

At decision time t , let \mathcal{S}_t denote the set of nodes (states) and $\{\pi_{t,s}\}_{s \in \mathcal{S}_t}$ the probabilities of those nodes, conditional on information at the start of period t . For any node-level variable $x_{t,s}$ ³, write its cross-node expectation as

$$(3) \quad x_t := \mathbb{E}_t[x_{t,S}] = \sum_{s \in \mathcal{S}_t} \pi_{t,s} x_{t,s}.$$

We summarize period t by the expected objects $\Phi_t := \mathbb{E}_t[\Phi_{t,S}]$ and $\kappa'_t := \mathbb{E}_t[\kappa'_{t,S}]$ when needed (using (3)).

The climate state at node (t, s) is $(C_{t,s}, \theta_{t,s})$, with $C_{t,s}$ and $\theta_{t,s}$ generated by Eqs. (A2)–(A3). Period- t expectations are $C_t := \mathbb{E}_t[C_{t,S}]$ and $\theta_t := \mathbb{E}_t[\theta_{t,S}]$. On the cost side, mitigation has node-specific marginal cost $\kappa'_{t,s}(m_{t,s}, L_{t,s})$, where $L_{t,s}$ indexes both exogenous technological progress and endogenous learning-by-doing. Past mitigation lowers future costs by shifting down the marginal cost curve.

III. Carbon price paths under delay

To test the cost of delay, we impose a zero-mitigation constraint for the first decision node and vary the length L of that period by shifting the initial decision time between 5, 10, and 15 years: $L \in \{5, 10, 15\}$. Each constrained run is then evaluated against two baseline scenarios, depending on the figure—the optimal

³Subscript (t, s) denotes a node-level object; subscript t alone denotes its period- t expectation across $s \in \mathcal{S}_t$ with weights $\pi_{t,s}$.

110 expected price at the same L , and one common $L = 10$ baseline. Figure 2 shows
 111 the resulting optimal carbon price paths in expectation over time. We here find
 112 that the carbon price paths in expectation of each delayed scenario lie above the
 113 baseline scenario's levels.⁴

114 If the optimum at time T_t is interior (i.e., $m_{t,s}^* \in (0, \bar{m})$ for all $s \in \mathcal{S}_t$) and
 115 baseline emissions $E_t > 0$, the first-order condition at each node equates the
 116 node-specific marginal abatement cost to the node-specific marginal damage:

$$(4) \quad \tau_{t,s} := \kappa'_{t,s}(m_{t,s}^*(\theta_{t,s}, L_{t,s}), L_{t,s}) = \Phi_{t,s}(\theta_{t,s}), \quad s \in \mathcal{S}_t.$$

117 where $\kappa'_{t,s}(m_{t,s}, L_{t,s}) = \partial \kappa_{t,s} / \partial m_{t,s}$. We summarize the decision period by the
 118 expected carbon price,

$$(5) \quad \tau_t := \mathbb{E}_t[\tau_{t,S}] = \mathbb{E}_t[\Phi_{t,S}(\theta_{t,S})] = \sum_{s \in \mathcal{S}_t} \pi_{t,s} \Phi_{t,s}(\theta_{t,s}),$$

119 which is the probability-weighted average across all nodes at time t . Learn-
 120 ing-by-doing and exogenous technological progress enter through $L_{t,s}$, shifting
 121 $\kappa'_{t,s}$ and thereby altering both the node-level prices $\tau_{t,s}$ and the expected price τ_t .

122 For period-level values, define the expected total mitigation cost and expected
 123 marginal abatement cost as $\kappa_t := \mathbb{E}_t[\kappa_{t,S}]$ and $\kappa'_t := \mathbb{E}_t[\kappa'_{t,S}]$. Note that be-
 124 cause $m_{t,s}$ is node-specific, $\kappa'_t \neq \partial \kappa_t / \partial m$ in general. At the node level, however,
 125 $\kappa'_{t,s}(m_{t,s}, L_{t,s}) = \partial \kappa_{t,s}(m_{t,s}, L_{t,s}) / \partial m_{t,s}$.

126 Delaying mitigation creates a deviation from optimal choice. By not allowing for
 127 mitigation for the first L years the world reaches the first unconstrained decision
 128 date $T_1 = L$ with a worse climate state: higher cumulative emissions, higher
 129 atmospheric CO₂ across persistence reservoirs, and higher temperatures. In that
 130 state, marginal damages are higher than they would have been without delay, and
 131 the representative agent's marginal willingness to pay to avoid one ton of CO₂,

⁴See Figure A1 for other outputs, like emissions and economic damages.

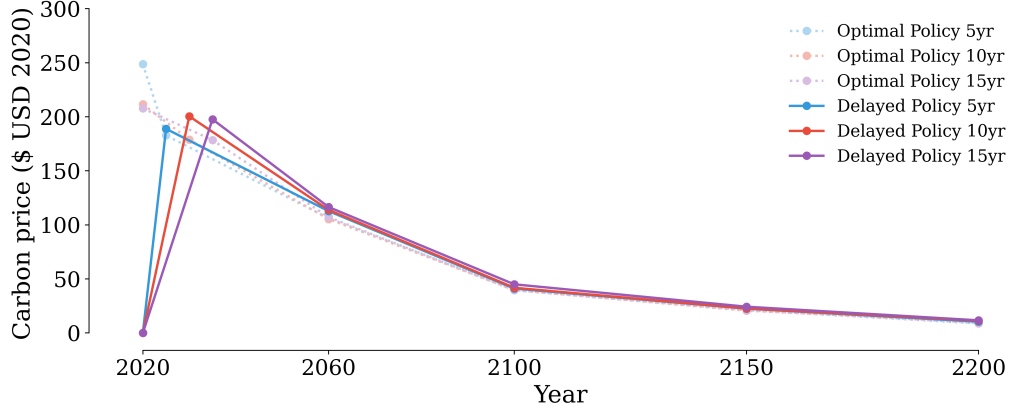


Figure 2. : Optimal CO₂-price paths under delayed policy implementation.

Note: Six decision times are used in all runs, but the length of the first decision period is varied between 5, 10, and 15 years, while all subsequent time steps remain fixed. Each delay scenario (5 yr, 10 yr, 15 yr) is solved as an independent run. We also show a canonical baseline scenario with a decision time at the 10-year step. The resulting carbon price paths show that postponing mitigation leads to a sharp upward adjustment in the first active period, followed by convergence toward the optimal no-delay trajectory.

132 $\Phi_L(\theta_L)$, is higher than it would have been without delay.

133 Worse still, delaying mitigation also means postponing learning-by-doing. Forc-
 134 ing $m_t = 0$ in the early window removes that source of endogenous cost decline
 135 (see Proposition A.1). As a result, when the world begins to act optimally at
 136 $T_1 = L$, it faces both a more fragile climate state and a less mature—more
 137 expensive—abatement cost curve. The representative agent’s optimal response
 138 is therefore to start the policy period with a higher expected carbon price than
 139 in the no-delay baseline, and to immediately mitigate more aggressively. This
 140 jump in the required expected entry carbon price is structural: it comes from
 141 state dependence in climate damages and from foregone technological progress,
 142 not from a particular calibration of parameters.

143 Formally, under standard convexity of abatement costs and monotonicity of
 144 damages in the climate state (Appendix A.A1), the optimal expected carbon
 145 price at $T_1 = L$ in the delayed scenario, τ_L^{delay} , is weakly higher than the optimal
 146 expected carbon price at the same time in the no-delay baseline, τ_L^{base} , with
 147 strict inequality whenever the no-mitigation constraint was binding. The state-

Table 1—: Delay-to-price elasticity at re-entry

L (years)	Year	τ_L^{base}	τ_L^{delay}	$\Delta \log(\tau)$	$\eta(L)$ (%/yr)
5	2025	\$182.97	\$191.35	0.044810	0.896
10	2030	\$181.55	\$194.83	0.070607	0.706
15	2035	\$184.49	\$196.71	0.064150	0.428
Average					0.677

dependence logic is formalized in Proposition A.1 (Appendix A.A1).

We summarize the expected price impact with the delay-to-price elasticity

$$(6) \quad \eta(L) := \frac{\partial \log \tau_L^{\text{delay}}}{\partial L},$$

which is the percent increase in the required expected entry carbon price at the first unconstrained decision time per additional year of forced delay. Because our model is solved at discrete delay lengths only, we estimate $\eta(L)$ by finite differences using $L \in \{5, 10, 15\}$, i.e., $\eta(L) \approx (\log \tau_L^{\text{delay}} - \log \tau_L^{\text{base}})/L$.

Table 1 reports the resulting elasticities. For a 5-year delay, the required re-entry expected price rises from \$182.97 to \$191.35, which corresponds to about an 0.896% higher expected price per year of delay. For 10 and 15 years of delay, the effect remains positive but declines to 0.706% and 0.428% per year, respectively. Averaging across the three scenarios yields an elasticity of about 0.677% per year. A simple log-linear fit of the delayed expected prices on the delay length gives a smaller, global elasticity of 0.276% per year (SE: 0.000487), with a 95% confidence interval of [0.181%, 0.372%]. This confirms Proposition A.1: In every scenario we consider, a binding delay raises the required expected entry carbon price. The elasticity is declining in L , which implies a concave delay-price relationship: early years of inaction are disproportionately costly, as they push the system into a higher-damage (and technically, low-learning) state, while additional years of delay add to the carbon debt at a diminishing marginal rate.

As a robustness check, we also estimate a pooled delay-to-price elasticity across

the three scenarios by regressing the delayed re-entry expected price on the length of the delay,

$$(7) \quad \log(\tau_L^{\text{delay}}) = \alpha + \eta^{\text{OLS}} L + \varepsilon_L,$$

which yields $\widehat{\log(\tau_L^{\text{delay}})} = 5.2417 + 0.0028L$, with $R^2 = 0.97$. The slope coefficient $\eta^{\text{OLS}} = 0.0028$ implies that, on average across the 5-15 year range, each extra year of delay raises the required expected entry carbon price by about 0.276% per year. The 95% confidence interval corresponds to [0.181%, 0.372%] per year.

IV. Estimating deadweight losses (DWLs) of delay

To quantify the societal cost of delayed action, we compute the DWL associated with postponing mitigation. Specifically, we determine the additional consumption in the first period required to restore lifetime utility of the representative agent to the level of the unconstrained (baseline) case. Denoting baseline utility at the root as U_0^* , first-period consumption in the delayed scenario as c_0^D , and the expected (certainty-equivalent) future utility as $\text{CE}_1^D := (\mathbb{E}_0[U_1^\alpha])^{1/\alpha}$, we define the consumption-equivalent DWL $\phi \geq 0$ implicitly by

$$(8) \quad U_0^* = \left((1 - \beta)((1 + \phi)c_0^D)^\rho + \beta(\text{CE}_1^D)^\rho \right)^{1/\rho}.$$

Solving for ϕ yields⁵

$$(9) \quad \phi = \left[\frac{(U_0^*)^\rho - \beta(\text{CE}_1^D)^\rho}{(1 - \beta)(c_0^D)^\rho} \right]^{1/\rho} - 1, \quad (\rho \neq 0).$$

Applying this metric, we find that the DWL of delayed mitigation rises with the duration of inaction (Table 2). In our main specification, enforced bans on mitigation force higher entry expected carbon prices at $T_1 = L$, which we capture with the delay-to-price elasticity $\eta(L)$; that higher required expected starting price

⁵In the case of $\rho = 0$, we apply the Cobb-Douglas limit as derived in Appendix A.A2

Table 2—: Social cost of delaying climate action under alternative baselines

First period length L (years)	Canonical baseline		Aligned baseline		Difference (p.p.)
	DWL (%)	DWL (2020 USD tn)	DWL (%)	DWL (2020 USD tn)	
5	14.24	8.2	13.00	7.5	−1.24
10	21.82	12.6	21.87	12.7	+0.05
15	32.21	18.7	33.10	19.1	+0.89

Note: Deadweight loss (DWL) represents the consumption-equivalent compensation required for lifetime utility in the delayed-mitigation scenario to equal that in the corresponding baseline. The canonical baseline fixes the first decision period at 10 years across all runs to enable direct DWL comparisons. The aligned baseline matches each delay scenario to an unconstrained run with the same decision timeline (e.g., 5-year delay vs. 5-year baseline). The minor difference for the 10-year scenario reflects stochastic draws in the model’s Monte Carlo simulations. Dollar values are in trillions of 2020 USD.

187 translates directly into a larger consumption-equivalent DWL ϕ . In our main
 188 specification, banning mitigation for five years, ten years, and fifteen years pro-
 189 duces a DWL of delay of roughly 14%, 22%, and 32% of first-period consumption,
 190 respectively. In monetary terms, these correspond to about \$8.3tn, \$12.8tn, and
 191 \$18.8tn in one-time global compensation at the start of the policy window. Each
 192 additional year of delay raises the DWL by about \$1.05 trillion per year over the
 193 5–15 year range, i.e., roughly 1.8 percentage points of first-period consumption
 194 per year. A simple log-log fit implies $\phi(L) \propto L^{0.73}$, indicating sub-linear scaling
 195 and modestly declining marginal losses as the delay lengthens.

196 These DWLs increase with delay length, but not linearly. Longer bans on
 197 mitigation give the representative agent at the next decision time a more polluted
 198 atmosphere and therefore require a higher expected starting carbon price at $T_1 =$
 199 L under our standard assumptions. The agent then responds by catching up:
 200 once mitigation is finally allowed, the optimal policy sharply raises the expected
 201 carbon price at $T_1 = L$ relative to the no-delay baseline and moves immediately
 202 to very aggressive abatement. This catch-up behavior is economically painful in
 203 the short run, which shows up in $\phi(L)$, but it stabilizes the long run by limiting
 204 further deterioration of the climate-economy state. Numerically, in our baseline

calibration $\phi(L)$ rises quickly between 0 and 10 years of delay and continues to rise thereafter, though at a slower rate (Table 2). In our benchmark runs, then, the exogenously induced delay has a clearly measurable cost: for the 5-15 year range we study, every additional year without mitigation forces the social planner to start the policy period with an expected carbon price between about 0.4 and 0.9 percent higher than it otherwise would have been, with an average of 0.7 percent. The regression-based estimate is smaller because it smooths across the three scenarios, but it preserves the sign and the basic message: delay makes the first feasible expected carbon price higher.

Figure 3 examines the consequences of relaxing the stringency of the first-period policy constraint by imposing an upper bound $m(t) \leq p$ on the mitigation rate over the initial interval $t \in [0, L]$, where $p \in [0, 1]$ denotes the maximum share of baseline emissions that may be abated. For caps close to the unconstrained solution, the DWL increases approximately quadratically in the cap’s tightness, with the level of the loss rising in the duration of the delay L .

This quadratic relationship provides a simple heuristic for why even limited early mitigation recovers a disproportionate fraction of welfare, and why DWL converges rapidly to zero as p approaches the smallest nonbinding cap (and the constraint ceases to bind). Conversely, the marginal welfare gain from relaxing the constraint is decreasing in p .

V. Evaluating parameter importance

Understanding why delay is so costly requires unpacking which structural primitives make the carbon-debt difference $\tau_L^{\text{delay}} - \tau_L^{\text{base}}$ and its elasticity as per Equation (6) large, and therefore drive the DWL penalty ϕ . Figure 4 offers a first look, plotting the DWL of delay against four structural drivers: EIS, PRTP, exogenous technological change, and endogenous learning. Lines show within-delay OLS fits of the expected DWL on the parameter value. The fitted Gaussian curves show the distribution of $\phi(L)$ for the different delay lengths given our parameter space.

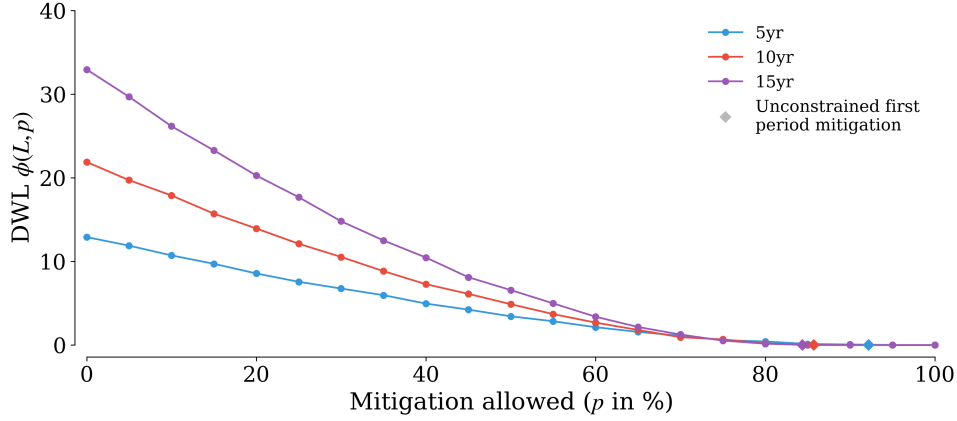


Figure 3. : DWL as a function of allowed partial mitigation p in the first period.

Note: Policies are compared under the aligned baseline in the main specification (see Appendix A.A1). Small variation in smoothness are due to the stochastic nature of the model.

233 The central result is that impatience dominates. When societies heavily discount
 234 the future, no amount of technological progress or learning can offset the welfare
 235 lost from postponing mitigation.

236 Parameter sensitivities in Table 3 show which economic mechanisms drive the
 237 DWL of delaying climate action in a multivariate regression, i.e., they show partial
 238 OLS effects within our parameter grid. We estimate these effects over a broad
 239 random draw of the model's structural parameters, each sampled independently
 240 from its prior probability distribution. This approach ensures that coefficients
 241 capture partial effects across the full range of plausible economic and technological
 242 states. Each parameter thus maps a structural assumption into an economic
 243 intuition about risk, time, and technology.

244 Higher risk aversion (RA) raises the shadow value of insurance against uncertain
 245 climate damages. A one-point increase in γ raises the DWL by roughly 0.25
 246 percentage points, or about \$147 billion. This result is highly significant. Agents
 247 who are risk-averse value early mitigation more strongly as protection against
 248 catastrophic tail outcomes. Nonetheless, RA across states of nature matters less
 249 than aversion across time (see EIS): what dominates is not which climate future

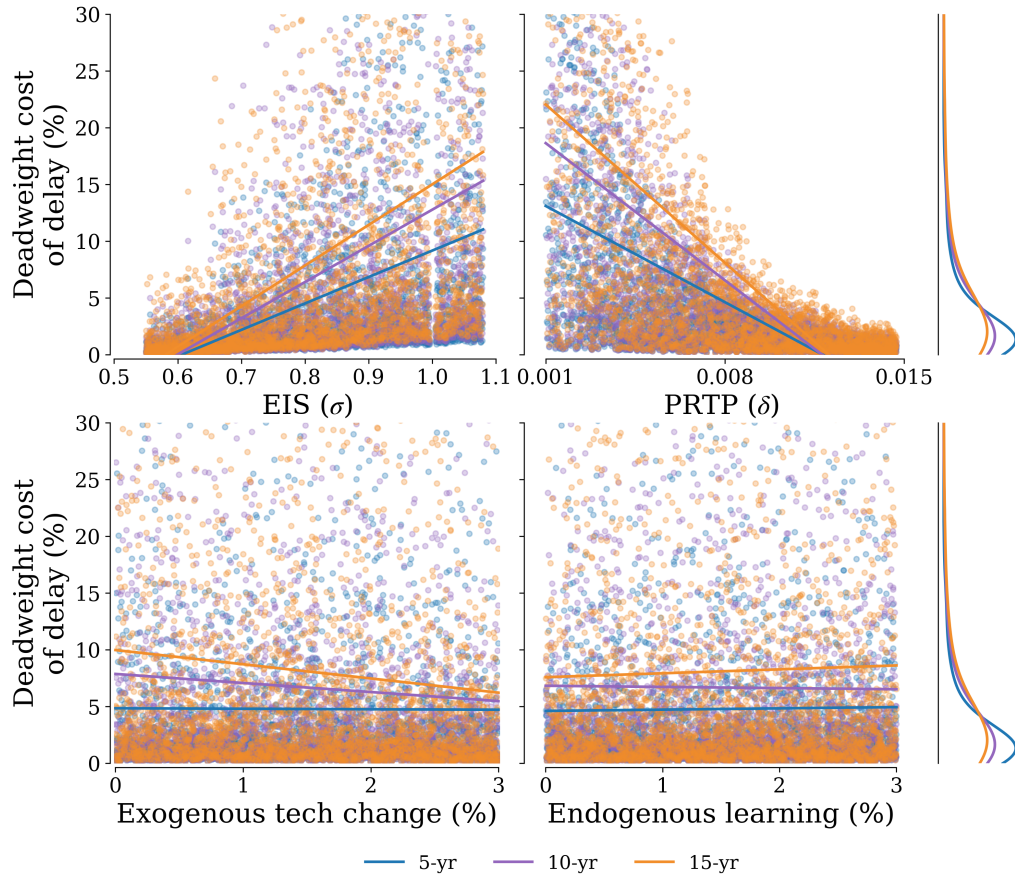


Figure 4. : Variance decomposition of deadweight losses (DWLs) by structural parameters.

Note: The figure truncates the vertical axis at 30% to improve visibility. This range contains approximately 95% of observations.

occurs but how long society waits to act.

The elasticity of intertemporal substitution (EIS) is the single strongest behavioral determinant of delay costs. A 0.1 increase in σ (within the sampled range of 0.55-1.1) raises the DWL by about 5%, or \$3 trillion ($p < 0.001$). In the unconstrained baseline, such a society is willing to sacrifice some near-term consumption (via costly early mitigation) in exchange for much lower climate damages later. A binding delay prevents that optimal intertemporal trade, so the DWL $\phi(L)$ from delay is larger when σ is high.

Table 3—: Regression results: determinants of deadweight loss (DWL) and mitigation delay outcomes

	(1)	(2)	(3)
Const	-0.0457** (0.0199)	-10.5381 (8.3528)	-6301.7279 (4994.9064)
RA (γ)	0.0046*** (0.0002)	0.2454*** (0.0847)	146.7690*** (50.6514)
EIS (σ)	0.4767*** (0.0057)	49.7372*** (2.5267)	29742.5249*** (1510.9441)
Tech. change (exog.)	-1.4735*** (0.0935)	-73.5360* (38.5723)	-43974.0590* (23066.0244)
Tech. learning (endo.)	0.8882*** (0.0883)	63.7416* (34.3644)	38117.0615* (20549.6858)
PRTP (δ)	-23.5410*** (0.2509)	-2556.3668*** (111.3807)	-1528691.37*** (66604.948)
log(Backstop premium)	-0.0009 (0.0020)	-0.6235 (0.8472)	-372.8457 (506.6172)
Cons. growth	-3.5662*** (0.1814)	-57.4224 (77.6601)	-34338.2212 (46440.2569)
Delay 10	0.0469*** (0.0015)	3.4608*** (0.3973)	2069.5203*** (237.5642)
Delay 15	0.1088*** (0.0021)	8.5027*** (0.7598)	5084.5728*** (454.3852)
R ²	0.7639	0.2034	0.2034
Adj. R ²	0.7636	0.2026	0.2026
N	8830	8830	8830

Note: Results from an OLS regression with time fixed effects (Delay 10 and 15). Heteroskedasticity-robust standard errors in parentheses. All specifications include the same nine regressors. Delay 10 and Delay 15 are indicator variables for the different delay periods and reference delay 5. The dependent variable in column (1) is the utility loss (in %) from delaying optimal climate policy. Column (2) uses the consumption-equivalent DWL ($\phi(L)$ in %), and column (3) uses the absolute DWL in billions of 2020 USD.

*** $p < 0.01$, ** $p < 0.05$, * $p < 0.1$.

258 With a negative coefficient significant at the 10% level, faster exogenous tech-
259 nological change cushions the economy against delay. A one percentage-point
260 increase in the exogenous rate of technological change reduces DWL by roughly
261 0.7%, or about \$440 billion. Independent innovation lowers future abatement
262 costs and partially offsets delay. When technology improves independently of

early action, postponement hurts less because future abatement is cheaper. Conversely, technological stagnation amplifies the cost of delay.

Endogenous technological learning has a positive coefficient that is significant at the 10% level with similar magnitude to exogenous change. A one percentage-point increase in learning intensity raises DWL by about 0.6%, or \$380 billion. The mechanism is path dependence: delaying mitigation slows learning-by-doing, delaying cost reductions and locking in higher future abatement costs. Inaction today undermines tomorrow's productivity gains.

The pure rate of time preference (PRTP, δ) has a large and statistically significant effect. The coefficient implies that raising δ by 1 percentage point lowers DWL by roughly 25.6 percentage points, or \$ 15.3 trillion. More impatient societies (higher δ , lower β) care relatively less about distant future damages. In our regressions, this shows up as a lower measured DWL from delay. Conversely, patient societies (low δ) view delay as extremely expensive. This confirms that how we value time, not technology or static risk, is a first-order driver of the DWL variation across scenarios.

The backstop premium, that is, the long-run cost ceiling for zero-carbon technology, is statistically insignificant and economically negligible. A 1% change in the backstop price shifts DWL by less than 0.01%, or about \$0.4 billion. In the model, this parameter adds a surcharge to the marginal cost of over-mitigation, that is, for mitigation levels above 100%, corresponding to net carbon removal. This captures the real-world cost gap between eliminating emissions and achieving net-negative emissions through technologies such as direct air capture. Because optimal policy paths in our delay experiments rarely enter the over-mitigation regime, the DWL effects of the premium remain small.

Consumption growth enters negatively. A 1-percentage-point faster consumption-growth rate reduces the DWL by about 0.6%, or \$340 billion. Even though it is not significant, the sign aligns with the theoretical expectation that faster growth decreases the DWL of delay.

292 Both delay length indicator variables are positive and highly significant. Ex-
293 tending the first decision period from 5 to 10 years raises the DWL by about
294 3.5%, or \$2.1 trillion; extending to 15 years increases them by roughly 8.5%, or
295 \$5.1 trillion. The rise is steep but concave, consistent with the model's adaptive
296 catch-up dynamics: once mitigation begins, expected carbon prices jump sharply,
297 partially—but never fully—recovering lost welfare.

298 Taken together, our analysis shows that the economics of delay is fundamentally
299 about time preference and intertemporal trade-offs: Impatience and substitution,
300 not technology or risk, explain most of the DWL of inaction, underscoring that
301 the true price of delay is paid in lost time.

REFERENCES

- Ackerman, Frank, Elizabeth A Stanton, and Ramón Bueno. 2013. “Epstein–Zin utility in DICE: Is risk aversion irrelevant to climate policy?” *Environmental and Resource Economics*, 56(1): 73–84.
- Bauer, Adam Michael, Cristian Proistosescu, and Gernot Wagner. 2024. “Carbon Dioxide as a Risky Asset.” *Climatic Change*, 177(5): 72.
- Bertram, Christoph, Elina Brutschin, Laurent Drouet, Gunnar Luderer, Bas van Ruijven, Lara Aleluia Reis, Luiz Bernardo Baptista, Harmen-Sytze de Boer, Ryna Cui, Vassilis Daioglou, et al. 2024. “Feasibility of peak temperature targets in light of institutional constraints.” *Nature Climate Change*, 14(9): 954–960.
- Bilal, Adrien, and Diego R Känzig. 2025. “The macroeconomic impact of climate change: Global vs. local temperature.” National Bureau of Economic Research.
- Burke, Marshall, Solomon M. Hsiang, and Edward Miguel. 2015. “Global non-linear effect of temperature on economic production.” *Nature*, 527(7577): 235–239.
- Burke, Marshall, W. Matthew Davis, and Noah S. Diffenbaugh. 2018. “Large potential reduction in economic damages under UN mitigation targets.” *Nature*, 557(7706): 549–553.
- Clausing, Kimberly A., Christopher R. Knittel, and Catherine Wolfram. 2025. “Who Bears the Burden of Climate Inaction?”
- Daniel, Kent D., Robert B. Litterman, and Gernot Wagner. 2019. “Declining CO₂ price paths.” *Proceedings of the National Academy of Sciences*, 116(42): 20886–20891.

- 327 **Dechezleprêtre, Antoine, Adrien Fabre, Tobias Kruse, Bluebery**
328 **Planterose, Ana Sanchez Chico, and Stefanie Stantcheva.** 2025. “Fight-
329 ing climate change: International attitudes toward climate policies.” *American*
330 *Economic Review*, 115(4): 1258–1300.
- 331 **Dietz, Simon, James Rising, Tobias Stoerk, and Gernot Wagner.** 2021.
332 “Economic impacts of tipping points in the climate system.” *Proceedings of the*
333 *National Academy of Sciences*, 118(34): e2103081118.
- 334 **Epstein, Larry G, and Stanley E Zin.** 1989. “Substitution, Risk Aversion,
335 and the Temporal Behavior of Consumption and Asset Returns: A Theoretical
336 Framework.” *Econometrica: Journal of the Econometric Society*, 937–969.
- 337 **Epstein, Larry G, and Stanley E Zin.** 1991. “Substitution, risk aversion, and
338 the temporal behavior of consumption and asset returns: An empirical analysis.”
339 *Journal of political Economy*, 99(2): 263–286.
- 340 **Howard, Peter H., and Thomas Sterner.** 2017. “Few and Not So Far Be-
341 tween: A Meta-analysis of Climate Damage Estimates.” *Environmental and Re-*
342 *source Economics*, 68(1): 197–225.
- 343 **Intergovernmental Panel on Climate Change (IPCC).** 2023. “Climate
344 Change 2023: Synthesis Report. Contribution of Working Groups I, II and III to
345 the Sixth Assessment Report of the Intergovernmental Panel on Climate Change.”
346 Intergovernmental Panel on Climate Change (IPCC), Geneva, Switzerland.
- 347 **Joos, F., R. Roth, J. S. Fuglestvedt, G. P. Peters, I. G. Enting, W. von**
348 **Bloh, V. Brovkin, E. J. Burke, M. Eby, N. R. Edwards, T. Friedrich,**
349 **T. L. Frölicher, P. R. Halloran, P. B. Holden, C. Jones, T. Kleinen,**
350 **F. T. Mackenzie, K. Matsumoto, M. Meinshausen, G.-K. Plattner, A.**
351 **Reisinger, J. Segschneider, G. Shaffer, M. Steinacher, K. Strassmann,**
352 **K. Tanaka, A. Timmermann, and A. J. Weaver.** 2013. “Carbon dioxide and

climate impulse response functions for the computation of greenhouse gas metrics:
a multi-model analysis.” *Atmospheric Chemistry and Physics*, 13(5): 2793–2825.

Lemoine, Derek, and Christian Traeger. 2014. “Watch your step: optimal policy in a tipping climate.” *American Economic Journal: Economic Policy*, 6(1): 137–166.

Meckling, Jonas. 2025. “The geoeconomic turn in decarbonization.” *Nature*, 645(8082): 869–876.

Meckling, Jonas, Thomas Sterner, and Gernot Wagner. 2017. “Policy sequencing toward decarbonization.” *Nature Energy*, 2(12): 918–922.

Mildenberger, Matto. 2020. *Carbon captured: How business and labor control climate politics*. MIT Press.

Mildenberger, Matto, and Dustin Tingley. 2019. “Beliefs about climate beliefs: the importance of second-order opinions for climate politics.” *British Journal of Political Science*, 49(4): 1279–1307.

Moore, Frances C, Moritz A Drupp, James Rising, Simon Dietz, Ivan Rudik, and Gernot Wagner. 2024. “Synthesis of evidence yields high social cost of carbon due to structural model variation and uncertainties.” *Proceedings of the National Academy of Sciences*, 121(52): e2410733121.

Oreskes, Naomi, and Erik M Conway. 2011. *Merchants of doubt: How a handful of scientists obscured the truth on issues from tobacco smoke to global warming*. Bloomsbury Publishing USA.

Rose, Steven K., Delavane B. Diaz, and Geoffrey J. Blanford. 2017. “Understanding the Social Cost of Carbon: A Model Diagnostic and Inter-comparison Study.” *Climate Change Economics*, 8(02): 1750009.

Stechemesser, Annika, Nicolas Koch, Ebba Mark, Elina Dilger, Patrick Klösel, Laura Menicacci, Daniel Nachtigall, Felix Pretis, Nolan Ritter,

- 379 **Moritz Schwarz, et al.** 2024. “Climate policies that achieved major emission
380 reductions: Global evidence from two decades.” *Science*, 385(6711): 884–892.
- 381 **Traeger, Christian P.** 2014. “Why uncertainty matters: discounting under
382 intertemporal risk aversion and ambiguity.” *Economic Theory*, 56(3): 627–664.
- 383 **Wagner, Gernot, and Richard J Zeckhauser.** 2012. “Climate policy: hard
384 problem, soft thinking.” *Climatic change*, 110(3): 507–521.

A1. Model and dynamics

This section formally describes the model setup and proves Proposition A.1. Decisions occur on a finite set of times T_0, T_1, \dots, T_N , measured in calendar years (e.g., $T_0 = 2020, T_1 \in \{2025, 2030, 2035\}$, etc.). At each decision time T_t and node, the social planner (our representative agent) chooses the mitigation rate $m_t \in [0, \bar{m}]$ that applies over the entire subsequent interval $[T_t, T_{t+1})$. Values $m_t > 1$ are net removal of CO₂ (direct air capture and related negative-emissions technologies) at a backstop premium. In our benchmark calibration, $\bar{m} = 1.5$ and the backstop premium is \$10,000.

Following Daniel, Litterman and Wagner (2019), we embed the planner in a non-recombining binomial tree in which each node inherits a current fragility state that indexes how severe climate damages have turned out so far. The high-fragility branches correspond to high realized damages (or bad climate/economic states), and the low-fragility branch to more benign outcomes. Uncertainty therefore resolves gradually along the tree rather than all at once. At each node, the agent re-optimizes given the currently realized state.

This structure matters for two reasons. First, it makes the problem explicitly stochastic as future consumption, temperature, and damages differ across branches. Second, it allows us to separate aversion to risk across time from aversion to risk across states of nature. The same structure also lets us impose politically relevant constraints on early climate policy: we can constrain the agent not to mitigate for an initial window and then ask how the system behaves once the constraint is lifted.

We analyze delays in mitigation by imposing an exogenous no-mitigation period of length L years. Formally, for a given $L \in \{5, 10, 15\}$, we impose $m_t = 0$ for all decision times $T_t < L$, and relax this constraint for $T_t \geq L$.⁶ We compare each

⁶In our standard calibration, this corresponds to constraining T_0 only.

412 scenario to a common unconstrained baseline with a node at $T_t = 10$ in which
 413 the planner is free to choose m_t at all decision times.

414 Preferences follow a standard Epstein-Zin recursive specification as in Equa-
 415 tion (1) with terminal utility given by Equation (2). For our main specification,
 416 parameter values are as follows: $\text{PRTP}(\delta) = 0.002$; $\text{EIS}(\sigma) = 0.833$; $\text{RA}(\gamma) = 10$;
 417 consumption growth p.a. = 0.02; exog. tech change = 0.015; endo. tech learning =
 418 0; baseline emissions = SSP2; backstop premium = 10 000.

419 EMISSIONS, CLIMATE DYNAMICS, COSTS, AND DAMAGES

420 For expositional clarity, throughout this subsection we fix an arbitrary realiza-
 421 tion (i.e., path) of uncertainty and suppress state indices; all objects $(m_t, \theta_t, L_t, \kappa_t, \Phi_t, \tau_t)$
 422 are thus defined along a single path in our binomial tree.

423 Let $E_t > 0$ denote the baseline (business-as-usual) CO_2 emissions over the
 424 interval $[T_t, T_{t+1})$, based on a reference socioeconomic pathway (e.g., SSP2). The
 425 planner can abate a fraction $m_t \in [0, \bar{m}]$ of those baseline emissions, so realized
 426 emissions over that interval are

$$(A1) \quad e_t = (1 - m_t)E_t.$$

427 The climate state at time T_t is characterized by two key variables: atmospheric
 428 CO_2 concentration C_t (in ppm) and temperature anomaly θ_t (in $^\circ\text{C}$ above prein-
 429 dustrial).

430 Atmospheric CO_2 concentration C_t evolves as the convolution of past emissions
 431 with the impulse response function (IRF) of the carbon cycle, following Joos et al.
 432 (2013):

$$(A2) \quad C_t = C_0 + \chi \int_0^t \Psi(t-s)e_s ds, \quad \text{where } \Psi(s) = a_0 + \sum_{i=1}^3 a_i \exp(-s/b_i),$$

433 with $\chi = 1/7.8 = 0.128$ ppm/Gt CO_2 and coefficients $a_0 = 0.2173$, $a_1 = 0.2240$,

434 $a_2 = 0.2824$, $a_3 = 0.2763$, and time constants $b_1 = 394.4$, $b_2 = 36.54$, $b_3 = 4.304$
 435 years. All $a_i, b_i > 0$, so concentrations are strictly increasing in cumulative
 436 emissions. These parameters capture the multiple carbon-cycle reservoirs (at-
 437 mosphere, mixed-layer ocean, deep ocean, biosphere) and the long-lived airborne
 438 fraction a_0 .

439 The global mean surface temperature anomaly θ_t is linked to cumulative emis-
 440 sions through the Transient Climate Response to Cumulative Emissions (TCRE)
 441 framework following AR6:

$$(A3) \quad \theta_t = \lambda_{\text{eff}} \int_0^t e_u du, \quad \lambda_{\text{eff}} := \frac{\lambda}{1 - f_{\text{nc}}}.$$

442 Here e_u denotes CO₂ emissions at time u measured in thousand gigatonnes of
 443 CO₂ per year (TtCO₂/yr), so that $\int_0^t e_u du$ is cumulative emissions in thousands
 444 GtCO₂. The parameter $\lambda > 0$ (in K per 1000 GtCO₂) is the TCRE for CO₂-
 445 only warming, while $f_{\text{nc}} \in (0, 1)$ scales in the contribution from non-CO₂ forcing.
 446 Following Bauer, Proistosescu and Wagner (2024), we take the effective TCRE to
 447 be $\lambda_{\text{eff}} \sim \mathcal{N}(0.52, 0.21^2)$ K per TtCO₂.

448 This formulation implies three key properties for our analytical results:

- 449 (i) C_t and θ_t are strictly increasing in the emissions path $\{e_s\}_{s \leq t}$ because
 450 $\Psi(\zeta) \geq 0$ and $\lambda_{\text{eff}} > 0$.
- 451 (ii) The multi-timescale IRF ensures that past emissions affect concentrations
 452 far into the future, with fraction a_0 remaining indefinitely.
- 453 (iii) High emissions in $[T_i, T_{i+1})$ permanently elevate both C_t and θ_t for all sub-
 454 sequent times.

455 Based on Burke, Davis and Diffenbaugh (2018); Rose, Diaz and Blanford (2017);
 456 Howard and Sterner (2017); Dietz et al. (2021), damages are represented as the
 457 sum of an aggregate temperature-based loss component and an additional com-

458 ponent from climate tipping points:

$$(A4) \quad d_t = D^{(k)}(\theta_t) + d_{\text{tp}}(\theta_t), \quad D^{(k)}(\theta_t) = \delta_1^{(k)}\theta_t + \delta_2^{(k)}\theta_t^2$$

459 where $k \in \{\text{statistical, structural, meta}\}$ indexes the aggregate damage family,
 460 and $d_{\text{tp}}(\theta_t)$ captures the expected effect of climate tipping events. The coefficients
 461 $(\delta_1^{(k)}, \delta_2^{(k)})$ were calibrated by (Bauer, Proistosescu and Wagner, 2024) from the
 462 respective sources and may vary across periods⁷, but for any fixed t , each $D^{(k)}$ is
 463 quadratic in θ_t and increasing on the temperature range we study (0-6°C).

464 The structural IAM function (Rose, Diaz and Blanford, 2017) and the meta-
 465 analytic function (Howard and Sterner, 2017) are convex ($\delta_{2,t}^{(\cdot)} > 0$) over our
 466 calibration. The statistical function (Burke, Hsiang and Miguel, 2015) is convex
 467 through mid-century and becomes mildly concave in late-century ($\delta_{2,t}^{(\text{stat})} < 0$ for t
 468 after 2100) but remains increasing on the relevant temperature range. The tipping
 469 component $d_{\text{tp}}(\theta_t)$ is also quadratic with positive curvature (Dietz et al., 2021),
 470 so it raises marginal damages at higher temperatures. To not rely too heavily
 471 on single estimates, our main specification averages across the three aggregate
 472 families with equal probability and adds the tipping component in every draw.
 473 Hence, we define the model-averaged damages at time t as

$$(A5) \quad \bar{D}(\theta_t) := \mathbb{E}_k \left[D^{(k)}(\theta_t) + d_{\text{tp}}(\theta_t) \right] \quad \forall k,$$

474 where the expectation is over the three aggregate families with equal weights. In
 475 our main specification, this means $\bar{D}(\theta_t)$ is twice continuously differentiable and
 476 satisfies

$$(A6) \quad \frac{d\bar{D}(\theta_t)}{d\theta_t} > 0 \quad \text{and} \quad \frac{d^2\bar{D}(\theta_t)}{d\theta_t^2} \geq 0$$

⁷The statistical specification from (Burke, Hsiang and Miguel, 2015), for example, uses distinct mid- and end-century calibration.

477 for temperatures between 0 and 6 °C.

478 The period- t marginal abatement cost curve (MACC) follows the exponential
 479 form and is calibrated to IPCC AR6 Working Group III data (Intergovernmen-
 480 tal Panel on Climate Change , IPCC), consistent with Bauer, Proistosescu and
 481 Wagner (2024). For a mitigation rate $m_t \in [0, \bar{m}]$ and technology and learning
 482 state L_t , which captures both exogenous and endogenous technological progress,
 483 we specify

$$(A7) \quad \tau_t(m_t, L_t) = \begin{cases} L_t \tau_0 (e^{\xi m_t} - 1), & 0 \leq m_t \leq 1, \\ L_t (\tau_0 + \tau^{\text{prem}}) (e^{\xi m_t} - 1), & m_t > 1, \end{cases}$$

484 where $\tau_0 > 0$ and $\xi > 0$ are level and curvature parameters, and $\tau^{\text{prem}} > 0$ is a
 485 backstop premium representing the additional cost of net-negative emissions (e.g.,
 486 direct air capture). The corresponding total mitigation cost function is obtained
 487 by integrating the marginal cost curve for $m_t \leq 1$,

$$(A8) \quad \kappa_t(m_t, L_t) = L_t \tau_0 \left(\frac{e^{\xi m_t} - 1}{\xi} - m_t \right), \quad (0 \leq m_t \leq 1),$$

488 and analogously with $\tau_0 + \tau^{\text{prem}}$ for $m_t > 1$.⁸ On each regime $m_t \in [0, 1]$ and
 489 $m_t > 1$, the function $\kappa_t(\cdot, \cdot)$ is twice continuously differentiable, strictly increasing
 490 and convex in m_t , and weakly increasing in the learning factor L_t . Higher L_t
 491 indicates less technological progress and therefore higher costs, while lower L_t
 492 reflects learning-by-doing and innovation that shift the MACC downward.

493 The learning factor L_t evolves according to cumulative mitigation experience
 494 and exogenous technological improvement. Hence,

$$(A9) \quad L_t = (1 - \psi_0 - \psi_1 X_t)^{(Y_t - Y_{\text{ref}})},$$

495 where Y_t is the calendar year at decision time T_t , Y_{ref} is the reference year used

⁸Note that this creates a level jump at $m_t = 1$.

for calibration (2030 in our baseline), and parameters $\psi_0 \geq 0$ and $\psi_1 \geq 0$ capture exogenous and endogenous technological progress, respectively. The term X_t represents the weighted average mitigation up to time t ,

$$(A10) \quad X_t := \frac{\int_0^t m(\zeta)E(\zeta)d\zeta}{\int_0^t E(\zeta)d\zeta},$$

so that stronger cumulative mitigation or faster exogenous innovation lowers L_t and thereby reduces future abatement costs.

Let y_t be gross resources available for consumption at time T_t . Actual consumption is then determined by

$$(A11) \quad c_t = y_t - \kappa_t(m_t, L_t) - d_t(\theta_t).$$

Delay thus reduces consumption through a more deteriorated climate state causing higher damages, and slower cost decline raising mitigation costs.

OPTIMAL EXPECTED CARBON PRICES

To compare policies at a given decision time t , we now take expectations across nodes, as in the main text (see Equation (3)).

Proposition A.1. (Delay raises the expected entry carbon price) *Assume baseline emissions are strictly positive in all periods prior to T_1 , i.e., $E_t > 0$ for all $T_t < T_1$. Suppose:*

- (i) *The delay constraint is binding in the baseline period, i.e., there exists $t < T_1$ with $m_t^{base} > 0$, while in the delayed scenario $m_t^{delay} = 0$ for all $T_t < T_1$;*
- (ii) *The carbon-cycle and TCRE mappings in (A2)–(A3) satisfy $\Psi(\zeta) \geq 0$ and $\lambda_{eff} > 0$, so climate dynamics are monotone;*
- (iii) *Model-averaged damages are increasing and weakly convex: $\bar{D}'(\theta) > 0$ and $\bar{D}''(\theta) \geq 0$ (cf. (A5));*

517 (iv) The optimal m_{T_1} is interior in both the base and delay scenarios.

518 Then, for every node $s \in \mathcal{S}_{T_1}$, $\tau_{T_1,s}^{\text{delay}} \geq \tau_{T_1,s}^{\text{base}}$, and therefore, taking expectations
 519 across nodes,

$$(A12) \quad \tau_1^{\text{delay}} \geq \tau_1^{\text{base}},$$

520 with strict inequality whenever $\theta_{T_1,s}^{\text{delay}} > \theta_{T_1,s}^{\text{base}}$ on a set of nodes with positive prob-
 521 ability (equivalently, when $\mathbb{E}_1[\theta_{1,S}^{\text{delay}}] > \mathbb{E}_1[\theta_{1,S}^{\text{base}}]$).

522 *Proof.* Fix an arbitrary node $s \in \mathcal{S}_{T_1}$ and consider the unique history (path) lead-
 523 ing to s under the baseline and delayed scenarios. By construction, $m_t^{\text{delay}} = 0$ for
 524 all $T_t < T_1$, while by (i) there exists some $t < T_1$ with $m_t^{\text{base}} > 0$. From (A1), for
 525 at least one such t we have $e_t^{\text{delay}} = (1-0)E_t = E_t > (1-m_t^{\text{base}})E_t = e_t^{\text{base}}$. Hence
 526 cumulative emissions up to T_1 are (weakly) higher along the delayed path. By (ii)
 527 and the monotonicity of the carbon-cycle IRF and TCRE mappings (A2)–(A3),
 528 higher past emissions imply a (weakly) worse climate state at T_1 : $C_{T_1,s}^{\text{delay}} \geq C_{T_1,s}^{\text{base}}$
 529 and $\theta_{T_1,s}^{\text{delay}} \geq \theta_{T_1,s}^{\text{base}}$, with strict inequality if baseline mitigation was positive on
 530 a nonzero set. By (iii), marginal damages are increasing in temperature, so
 531 $\Phi_{T_1,s}(\theta_{T_1,s}^{\text{delay}}) \geq \Phi_{T_1,s}(\theta_{T_1,s}^{\text{base}})$, strictly when $\theta_{T_1,s}^{\text{delay}} > \theta_{T_1,s}^{\text{base}}$. Under the interior first-
 532 order condition at node (T_1, s) , $\tau_{T_1,s}^{\text{delay}} = \Phi_{T_1,s}(\theta_{T_1,s}^{\text{delay}})$ and $\tau_{T_1,s}^{\text{base}} = \Phi_{T_1,s}(\theta_{T_1,s}^{\text{base}})$,
 533 which implies the path-wise inequality $\tau_{T_1,s}^{\text{delay}} \geq \tau_{T_1,s}^{\text{base}}$. Taking expectations across
 534 nodes yields $\tau_1^{\text{delay}} = \mathbb{E}_{T_1}[\tau_{T_1,S}^{\text{delay}}] \geq \mathbb{E}_{T_1}[\tau_{T_1,S}^{\text{base}}] = \tau_1^{\text{base}}$, with strict inequality if
 535 $\theta_{T_1,s}^{\text{delay}} > \theta_{T_1,s}^{\text{base}}$ on a set of nodes with positive probability. Finally, delay implies
 536 a smaller technology stock (higher $L_{T_1,s}$) because learning-by-doing accumulates
 537 more slowly when early mitigation is zero. By (A9), $L_{T_1,s}^{\text{delay}} \geq L_{T_1,s}^{\text{base}}$, and since mit-
 538 igation costs are increasing in L_t , $\kappa_{T_1,s}(m_{T_1,s}, L_{T_1,s}^{\text{delay}}) \geq \kappa_{T_1,s}(m_{T_1,s}, L_{T_1,s}^{\text{base}})$. Hence
 539 the total resource cost under delay is weakly higher, reinforcing the conclusion
 540 that $\tau_1^{\text{delay}} \geq \tau_1^{\text{base}}$. \square

Table A1—: OLS estimate of the delay-to-price elasticity

	(1)
L (years)	0.002761 (0.000487)
Constant	5.241717 (0.004929)
R^2	0.969818
Observations	3

Note: Dependent variable: $\log(\tau_L^{\text{delay}})$. Robust standard errors in parentheses. 95% confidence interval for the slope: [0.001806, 0.003715], i.e. [0.181%, 0.372%] per year.

REGRESSION RESULTS DELAY-TO-PRICE ELASTICITY

A2. Analytical solutions

COBB-DOUGLAS LIMIT OF THE EZ AGGREGATOR AND THE FIRST PERIODIC
COMPENSATION

Solving for the consumption-equivalent DWL of delay when $\rho \neq 0$ is done in the main text. Here we consider the Cobb–Douglas case $\rho = 0$ (i.e. $\sigma = 1$).

As $\rho \rightarrow 0$, the Epstein–Zin aggregator $U_0 = ((1 - \beta)c_0^\rho + \beta \text{CE}_1^\rho)^{1/\rho}$ converges to the geometric (Cobb–Douglas) form $U_0 = c_0^{1-\beta} \text{CE}_1^\beta$. Let the delayed path have first-period consumption c_0^D and continuation certainty equivalent CE_1^D . We scale the first-period consumption by $(1 + \phi)$ and require the compensated delayed utility to equal the baseline utility U_0^* : $U_0^* = ((1 + \phi)c_0^D)^{1-\beta} (\text{CE}_1^D)^\beta$. Solving for ϕ gives the closed-form consumption-equivalent transfer:

$$(A13) \quad \phi_{\text{CD}} = \left[\frac{U_0^*}{(c_0^D)^{1-\beta} (\text{CE}_1^D)^\beta} \right]^{\frac{1}{1-\beta}} - 1.$$

A3. Extended outputs

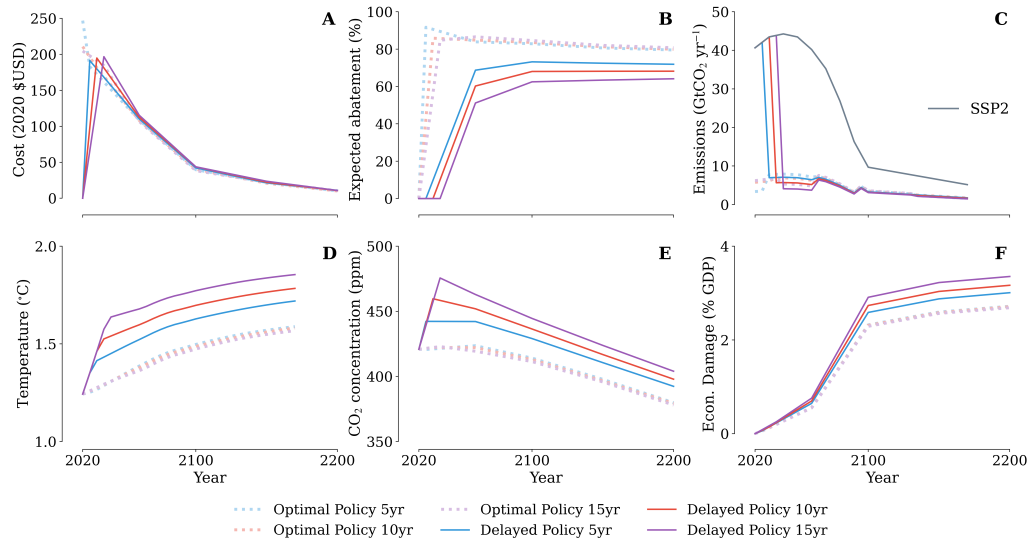
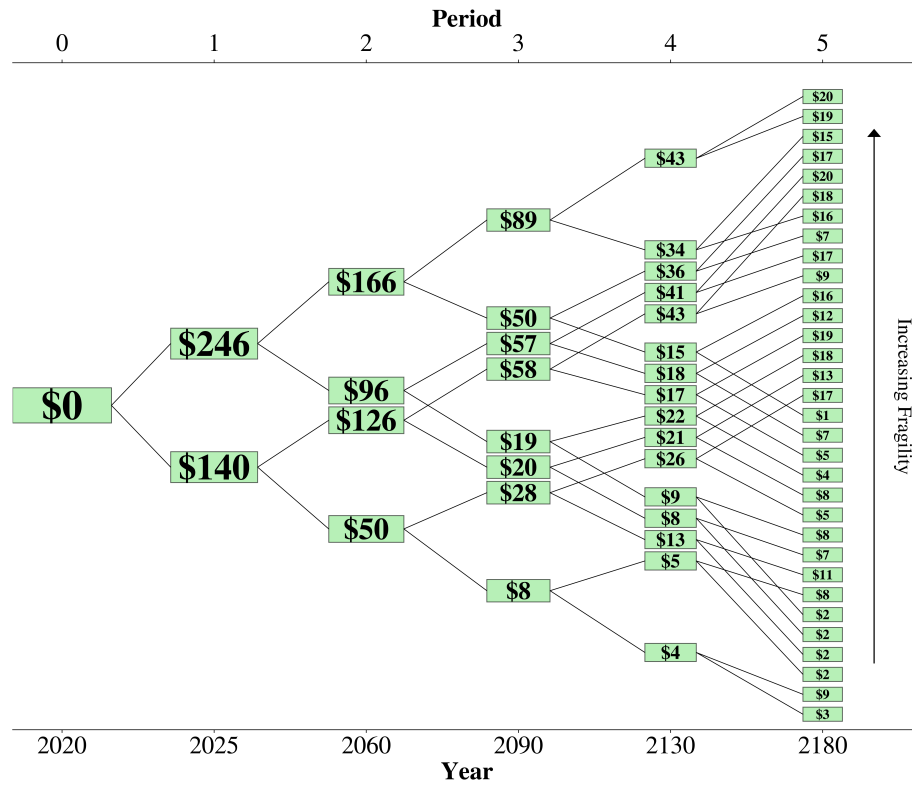
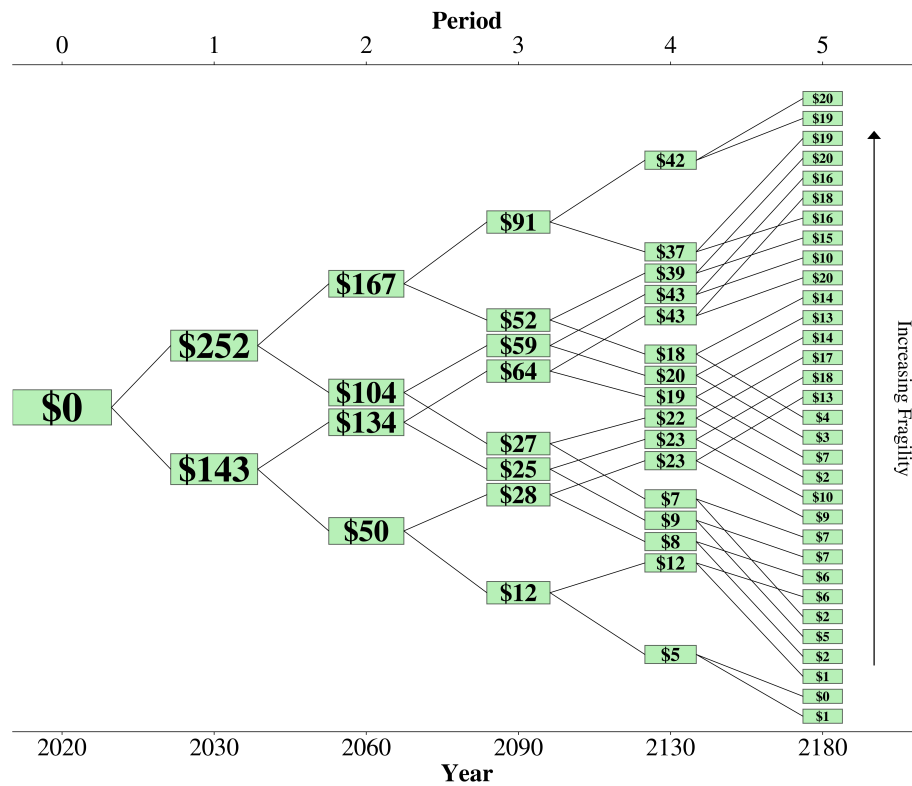


Figure A1. : Different outputs of the single-period optimal scenarios with delay periods $L \in \{5, 10, 15\}$.

Note: A: Expected carbon prices in 2020 $\$/\text{tCO}_2$. B: Expected abatement in %. C: Emissions in $\text{GtCO}_2/\text{year}$ with SSP2 emissions baseline. D: Temperature in degrees Celsius. E: CO_2 concentration in ppm. F: Economic damages in % of Gross Domestic Product.

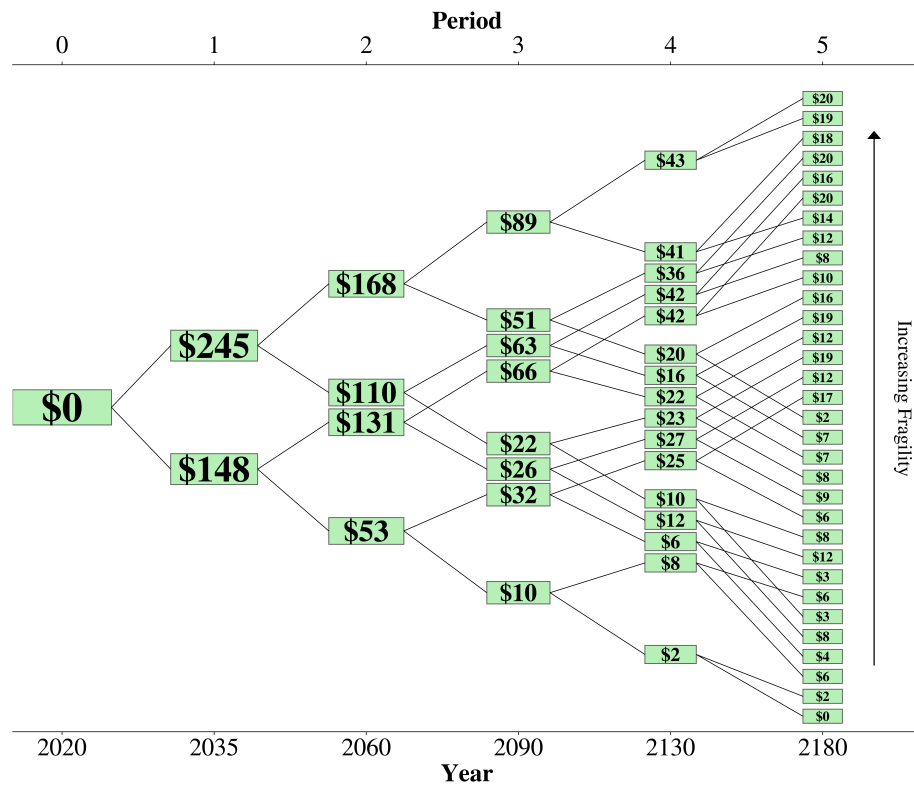


(a) Optimal price tree with 5-year delay.



(b) Optimal price tree with 10-year delay.

Figure A2. : Decision trees for delayed runs.



(c) Optimal price tree with 15-year delay.

Figure A2. : Decision trees for delayed runs (continued).